castcm2.doc
Miguel Castro-Colin: miguel@xray.phys.uh.edu
Wolfgang Donner: wdonner@uh.edu
Simon Moss: smoss@uh.edu
Zahirul Islam: zahir@aps.anl.gov
SRI-CAT
Sector 4
Material Science

Studies of the crystalline component within thin amorphous SiO$_2$ grown on Si(001)

M. Castro-Colin, [1] W. Donner, [1] S. C. Moss[1], Z. Islam[2]

[1]Physics Department, University of Houston, Houston, TX U.S.A.
[2]Argonne National Laboratory, Argonne, IL U.S.A.

Introduction

The system SiO$_2$/Si(001) has been sucessfully used over the years as a gate oxide [1]. In recent times the continuous thinning of this gate oxide has called the attention of numerous research teams, to investigate the behaviour of properties of the system when dimensions in the nanometer scale are used. A variety of studies have largely concentrated on defect generation in the oxide and its interfaces. The accumulation of these defects will degrade the performance of the gate oxide and lead to circuit failure. The basic idea behind gate oxide breakdown is that as stress time increases, traps build up in the oxide. Although some traps are charged, most of them are not, and it is only when the trap density reaches a critical level that a conduction path occurs and the oxide breakdown follows [2]. In turn the breakdown phenomenon is related to the distribution of localized states within the amorphous SiO$_2$, since these are understood to be responsible for the electrical, optical, and magnetic properties of amorphous solids [3]. Localized states are related to the very nature of the amorphous state [4, 5], in this case, that of SiO$_2$.

We have previously found, for the first time, in a series of experiments at 4-ID-D, that SiO$_2$ exhibits a depth-dependent amorphous structure factor, which is four-fold modulated through a symmetry imposed by the substrate, Si(001) [6]. This modulation is related to the volume fraction (about 0.1 %) of crystallites [7] registered within the amorphous matrix, through crystal truncation rod (CTR) measurements along Si(1 1 L) at L $\approx$ 0.45 (L = in reciprocal lattice units, r.l.u.) [6, 8, 9]. The crystallite occupancy has been modeled with an exponential function that vanishes towards the film surface [6, 8].

In the experiment currently discussed, we have searched for additional reflections that could aid in constructing a model of the SiO$_2$ crystalline phase found within the amorphous one. To this date, the models proposed, including ours [6], are based on a single reflection from the crystallites (1 1 0.45) [using Si as a reference]. The model favoured by our previous findings is that of distorted cristobalite, since its structure entails only a slight distortion of the SiO$_4$ tetrahedral units. In this experiment we have used a Buerger precession camera, a device able to collect, at once, data from extended regions of reciprocal space without distortion.

Scans using a diffractometer were also carried out, that yielded intensity at some of our predicted crystalline SiO$_2$ reflections.

Our results do not prove to be unambiguous, yet, at the same time, support our estimations [6] (and those of others [10,11]) that, strong static displacements (parallel to the film surface) of the atoms comprising the SiO$_2$ crystalline phase can hinder the appearance of further reflections.

Methods and Materials

The thin film samples investigated were prepared at N.C.S.U., with an RCA-clean that leaves a native oxide on the p-type Si(001)-oriented wafers from Okmetic. After being cleaned, the wafers were loaded into a tube furnace for thermal oxidation at 950 $^{\circ}$C for 66 minutes, to produce a 500 Å film (as measured from ellipsometry). Samples sizes of 1x5 mm and 10x10 mm were prepared for use in the precession camera, and diffractometer scans, respectively.

The Buerger precession camera (manufactured by Charles Supper) has been conditioned with an image plate (AGFA ADC-MD-30, 12 bit dynamic range), read off after exposure to X rays using a dentistry scanner Orex. The recording geometry of the precession camera makes it suitable to scan reciprocal space regions at a particular L position. L is selected through an appropriate combination setting of the circular slit diameter, slit-to-sample distance, and image-plate-to-sample distance [12]. Additionally we have added to the camera, a couple of circular pinholes of 0.5 mm diameter, to facilitate the camera alignment. The precession camera was placed on an optical bench already available at 4-ID-D, capable of motorized XYZ adjustments, for alignment purposes.

A wavelength of λ = 0.623 Å and a 0.2 mm beam diameter were used. The measurements consisted of scanning for about 60 to 300 seconds, each L selected. Camera parameters corresponding to the L values of 0, 0.1, 0.455, 0.5 0.7, 0.9, 1, and 1.2 r.l.u. were estimated to carry out the appropriate scans. Most scans were concentrated close to L = 0 r.l.u., since due to the static displacements, it is in that region were higher probability exists of detecting SiO$_2$ crystalline reflections.

For the diffractometer scans the same wavelength was used. To reduce the thermal diffuse scattering signal, the sample was placed inside a cryostat with a temperature down to about 10 K. With an incident angle of about 0.15°, several in-plane reflections were investigated.

Results

Figure 1 shows an image obtained exposing the image plate (IP) for 300 seconds. TDS intensity can be clearly observed spanning between reciprocal space positions. The centre of the image has a dark spot from which two prominent dark lines radially fan out (bottom region of Fig. 1); this is due to the
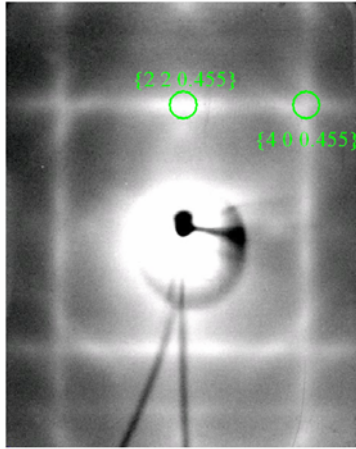
Fig. 1. Image collected with 300 seconds exposure, at L = 0.455. r.l.u. The TDS can aslo be observed (see [13] for comparison).

beam stop holder. The beam stop avoids photon saturation of the IP by the direct beam. Figure 1 displays the expected positions of {2 2 0.455} and {4 0 0.455}.

Figure 2, also at L = 0.455 r.l.u., exposed for 300 seconds, shows the TDS signal, as well as two other reflections at (1.58 0.67 0.455) and (1.60 0.67 0.455). Profiles obtained from the IP recordings, showed an intensity in the order of 0.13 counts per second (cps), at the indicated reflections.
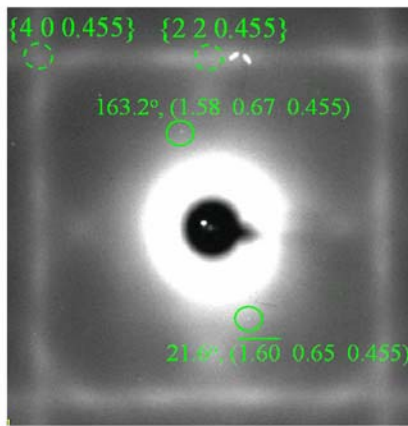

Fig. 2. After a slight tilt of the sample respect to the incoming beam, two reflections appear, as indicated. The TDS is also visible. The beamstop is the dark circle in the middle.

In Figure 3, the forbidden reflections {2 0 0} are excited in the sample[14-16]; at 60 seconds exposure. Two allowed reflections, (2 2 0) and (-2 -2 0), can also be appreciated; L = 0 in this case. Reflections (1.52 0.75 0) and (-1.52 0.75 0) are barely registered and additionally show some splitting due to misalignment of those particular reflections. In an image taken previous to that in Fig. 3, there was evidence that the sample was aligned such that (4 0 0) and (-4 0 0) presented an equal intensity within less than a percent difference, although the {2 2 0} reflections showed larger intensity discrepancy. By
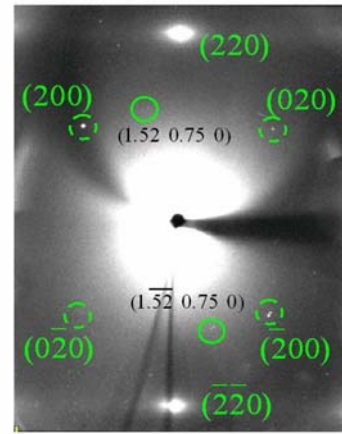

Fig. 3. Tilting of the sample permits the forbidden {2 0 0} reflections to arise, as well as two others, (1.52 0.75 0) and (-1.52 0.75 0). 60 sec. exposure.

reorienting the sample this way, the {2 0 0} reflections became visible, but their intensities were unequal.

On the other hand, measurements with the diffractometer, showed several reflections (purple squares), that are actually very close to those predicted (black squares) with the distorted coesite model, Fig. 4.

In Fig. 4 we have also included the positions corresponding to the Si{2 2 0} reflections, to have a better perspective of that region of reciprocal space.
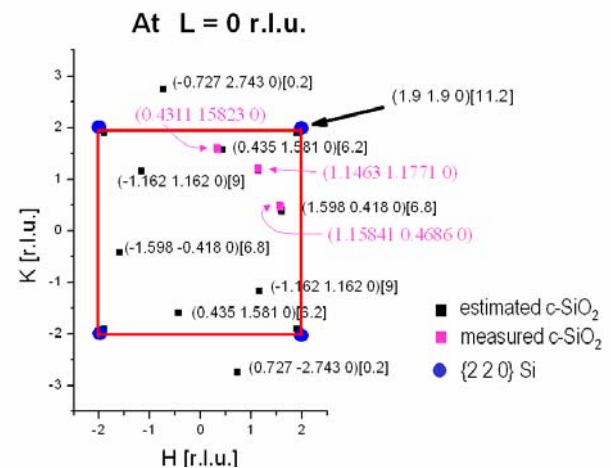

Fig. 4. The reflections obtained with the diffractometer (purple squares) are comparable with those estimated (black squares) from the model currently proposed. Expected relative intensities f the estimated reflections are also indicated within square brackets.

Discussion

Unfortunately it turned out to be a difficult task to properly align the precession camera to display the expected crystalline SiO_2 reflections. We could not confirm the existence of the in-plane (actually at L = 0.05 r.l.u.) reflections found with the diffractometer (Fig. 4) by using the camera. Even the weak reflections shown in Figs. 2 and 3, at fractional positions in reciprocal space were hard to focus, and hard to improve the

counting statistics, therefore their location is rather uncertain. Alternatively, reflections like those at {400}, {220}, {111} and {113} (these last two families are not shown here) were easily obtained without any splitting and with even intensities.

With the diffractometer itself, the use of the cryostat impeded to make a careful scan of the reflections found, in spite of the magnitude of the intensities (10^4 cps) registered. These reflections were only accessible by accomodating the sample at the radius, in Q space (momentum transfer space), corresponding to the estimated radius yielded by our model, and sucessively rotating the sample around the sample normal. Such geometry described a circular path in HK at a fixed L value. Therefore, in spite of the reasonable coincidence of the location between measured and estimated crystalline SiO_2 reflections, we can not yet confirm or discard our proposed pseudo-coesite model.

The splitting observed, for instance, in the reflections (1.52 0.75 0) and (-1.52 0.75 0), as previously indicated, is probably due to misalignment of those particular reflections; i.e., there is an offset of the plane that causes them, respect to L = 0 r.l.u.. An offset not only in the L direction but also in H and K. Two forbidden Si{2 0 0} reflections do not show any splitting, (2 0 0) and (0 2 0), but their intensities vary greatly, from saturation of the IP at (2 0 0), to about 15 cps at the (0 2 0), to absence in the (0 -2 0); additionally (-2 0 0) exhibits some splitting.

Further investigation is needed of the fractional reflections of Figs. 2 and 3 to understand their origin.

We would like to stress the importance of studying the structure of SiO_2, since this would, through appropriate modelling give a deeper insight into the defect generation in thin SiO_2, and thus, in the distribution of localized states. Thus bringing about the possibility of better models to explain the gate oxide breakdown upon thinning.

The precession camera showed to be a very good aid in displaying the TDS at various L planes. Our experiments produced images similar to those obtained by Holt et al. [13].

Acknowledgements

References

[1] C.J. Sofield and A.M. Stoneham, Semicond. Sci. Technol. **10**, 215 (1995).

[2] B. Riccó, M.Y. Azbel, and M.H. Brodsky. Phys. Rev. Lett. **51,** 1795 (1983).

[3] W. E. Spear, in *Amorphous and Liquid Semiconductors*, Ed. by J. Stuke and W. Brenig (Taylor and Francis LDT, London, 1974), pp 1.

[4] W. Y. Ching. Phys. Rev Lett. **46**, 607 (1981).

[5] J. Li and D. A. Drabold. Phys. Rev. B, **68**, 033103 (2003).

[6] M. Castro-Colin, W. Donner, S. C. Moss, Z. Islam *et al.* Submitted to Phys. Rev. B; accepted for publication (September 2004).

[7] F. Rochet, S. Rigo, M. Froment, *et al.* Adv. in Phys. **35**, 237 (1986).

[8] I. Takahashi, T. Shimura, and J. Harada. J. Phys.: Condens. Matter **5**, 6525 (1993).

[9] A. Munkholm., S. Brennan, F. Comin, and L. Ortega. Phys. Rev. Lett, **75**, 4254 (1995).

[10] K. Tatsumura, T. Watanabe, D. Yamasaki, *et al.* Phys. Rev. B **69**, 085212 (2004).

[11] A. Munkholm and S. Brennan, Phys. Rev. Lett. **93**, 036106 (2004).

[12] M. J. Buerger. *The photography of the reciprocal lattice.* Cambridge, Mass., The Murray printing company (1944).

[13] M. Holt, Z. Wu, H. Hong, et al. Phys. Rev. Lett. **83**, 3317 (1999).

[14] R. W. James, in The optical principles of the diffraction of X-rays. Oxbow Press, Woodbridge, Connecticut (1962), pp. 25,26, 339, 340.

[15] D. Mills, B. W. Batterman. Phys. Rev. B, **22**, 2887 (1980).

[16] E. Rossmanith. J. Appl. Cryst. **32**, 355 (1999).